NeuroImage 196 (2019) 152–160

Contents lists available at ScienceDirect

NeuroImage

journal homepage: www.elsevier.com/locate/neuroimage

Cardiovascular disease risk factors, tract-based structural connectomics, and cognition in older adults

Elizabeth A. Boots [a,b], Liang Zhan [c], Catherine Dion [d], Aimee J. Karstens [a], Jamie C. Peven [e], Olusola Ajilore [f], Melissa Lamar [a,b,g,*]

[a] Department of Psychology, University of Illinois at Chicago, Chicago, IL, 60607, USA
[b] Rush Alzheimer's Disease Center, Rush University Medical Center, Chicago, IL, 60612, USA
[c] Department of Electrical and Computer Engineering, University of Pittsburgh, Pittsburgh, PA, 15260, USA
[d] Department of Clinical and Health Psychology, University of Florida, Gainesville, FL, 32603, USA
[e] Department of Psychology, University of Pittsburgh, Pittsburgh, PA, 15260, USA
[f] Department of Psychiatry, University of Illinois at Chicago, Chicago, IL, 60612, USA
[g] Department of Behavioral Sciences, Rush University Medical Center, Chicago, IL, 60612, USA

ARTICLE INFO

Keywords:
Cardiovascular disease risk factors
Tract-based structural connectivity
Graph theory
Cognition
Dementia

ABSTRACT

Cardiovascular disease risk factors (CVD-RFs) are associated with decreased gray and white matter integrity and cognitive impairment in older adults. Less is known regarding the interplay between CVD-RFs, brain structural connectome integrity, and cognition. We examined whether CVD-RFs were associated with measures of tract-based structural connectivity in 94 non-demented/non-depressed older adults and if alterations in connectivity mediated associations between CVD-RFs and cognition. Participants (age = 68.2 years; 52.1% female; 46.8% Black) underwent CVD-RF assessment, MRI, and cognitive evaluation. Framingham 10-year stroke risk (FSRP-10) quantified CVD-RFs. Graph theory analysis integrated T1-derived gray matter regions of interest (ROIs; 23 a-priori ROIs associated with CVD-RFs and dementia), and diffusion MRI-derived white matter tractography into connectivity matrices analyzed for local efficiency and nodal strength. A principal component analysis resulted in three rotated factor scores reflecting executive function (EF; FAS, Trail Making Test (TMT) B-A, Letter-Number Sequencing, Matrix Reasoning); attention/information processing (AIP; TMT-A, TMT-Motor, Digit Symbol); and memory (CVLT-II Trials 1–5 Total, Delayed Free Recall, Recognition Discriminability). Linear regressions between FSRP-10 and connectome ROIs adjusting for word reading, intracranial volume, and white matter hyperintensities revealed negative associations with nodal strength in eight ROIs (p-values<.05) and negative associations with efficiency in two ROIs, and a positive association in one ROI (p-values<.05). There was mediation of bilateral hippocampal strength on FSRP-10 and AIP, and left rostral middle frontal gyrus strength on FSRP-10 and AIP and EF. Stroke risk plays differential roles in connectivity and cognition, suggesting the importance of multi-modal neuroimaging biomarkers in understanding age-related CVD-RF burden and brain-behavior.

1. Introduction

With no curative therapies currently available for Alzheimer's disease (AD) or related dementias, attention has shifted to identifying modifiable risk factors, such as cardiovascular disease risk factors (CVD-RFs), that could delay or even prevent the onset of dementia. Prior work has demonstrated that CVD-RFs are associated with both gray and white matter brain structures associated with risk for and development of dementia. For example, both hypertension (Beauchet et al., 2013; Firbank et al., 2007; Wiseman et al., 2004) and Type 2 diabetes mellitus (DM; Roberts et al., 2014) have been associated with less whole brain volume and decreases in hippocampal volumes in otherwise healthy older adults.

Abbreviations: AIP, Attention and Information Processing Speed; ANTs, Advanced Normalization Tools; BCT, Brain Connectivity Toolbox; BET, Brain Extraction Tool; CVD-RFs, Cardiovascular Disease Risk Factors; DM, Type 2 Diabetes Mellitus; FAS, Letter Fluency; FSRP-10, Framingham 10-Year Stroke Risk Profile; HAM-D, Hamilton Depression Rating Scale; LH, Left Hemisphere; PCA, Principal Component Analysis; PVIQ, Predicted Verbal Intelligence Quotient; RH, Right Hemisphere; ROIs, Regions of Interest; SMI, Subjective Memory Impairment; TMT, Trail Making Test; WTAR, Wechsler Test of Adult Reading.

* Corresponding author. Rush Alzheimer's Disease Center, Rush University Medical Center, 1750 W Harrison Street, Suite 1000, Chicago, IL, 60612, USA.
E-mail address: Melissa_Lamar@rush.edu (M. Lamar).

https://doi.org/10.1016/j.neuroimage.2019.04.024
Received 1 March 2019; Received in revised form 29 March 2019; Accepted 5 April 2019
Available online 10 April 2019

Additionally, lifespan studies examining a variety of CVD-RFs including hypertension, DM, smoking, and obesity found relationships between increased cardiovascular disease risk and decreased whole brain and hippocampal volumes, as well as alterations in frontal and posterior regions of the brain (Debette et al., 2011; Gonzales et al., 2017; Leritz et al., 2011). Likewise, hypertension and DM are associated with increased white matter hyperintensities (WMH), i.e., change of pallor in white matter as seen on T2-FLAIR scans (Debette et al., 2011; Iadecola et al., 2016; Meusel et al., 2014), as well as alterations in diffusion-tensor imaging (DTI) measures of white matter microstructural integrity (Gonzales et al., 2017; Hoogenboom et al., 2014; Jacobs et al., 2013; Kennedy and Raz, 2009; Wang et al., 2015). More specifically, hypertension, current smoking, and DM were all associated with worse white matter integrity in several white matter tracts including association and commissural tracts (de Groot et al., 2015), as well as the uncinate fasciculus, inferior and superior lateral fasciculi, and anterior thalamic radiation (McEvoy et al., 2015). However, less is known regarding the interplay of CVD-RFs with the structural integrity between gray matter regions (cortical and subcortical), and their connecting white matter.

Thus, while great strides have been made in understanding the impact of CVD-RFs in gray and white matter as they relate to cognition, a more integrated approach to understanding the tract-based structural connectivity between gray matter regions, subcortical structures, and connecting white matter is warranted (Iadecola, 2013). Initial work in this area has focused on the relationship between CVD-RFs and functional, rather than structural, connectivity. For example, a functional connectivity analysis revealed that compared with controls, hypertensive older adults had reduced frontal-parietal activity, which mediated the relationship between white matter integrity in the superior longitudinal fasciculi and executive function (Li et al., 2015). Thus far, however, there has been minimal work examining the structural connectivity of white matter and gray matter as it relates to CVD-RFs.

Advances in image analytics through the application of graph theory have made it possible to examine various structural connectivity indices that combine gray matter volumes and diffusion-weighted measures of white matter integrity (Rubinov and Sporns, 2010). These advanced neuroimaging methods allow analysis of brain structure in a more integrated form; for example, efficiency of local networks is determined by the path length (a proxy for white matter tracts) across nodes (or gray matter regions) within a region, and nodal strength of networks indicates the sum of the weights of the paths connected to a node. The application of these graph theory-based metrics to investigating the effect of CVD-RFs on structural connectivity is critical as it could help target areas vulnerable to cardiovascular dysfunction and signify biomarkers that could be targeted in prevention studies against cognitive decline.

This project investigated the associations between CVD-RFs, tract-based structural brain connectivity, and cognition. Not surprisingly given the role CVD-RFs play in brain gray and white matter alterations, there is a large literature outlining the effect of these same risk factors on cognitive function (Iadecola et al., 2016; Lamar et al., 2015), particularly in domains of executive function (Elias et al., 2004), processing speed (Llewellyn et al., 2008), and to a lesser extent, memory (Gifford et al., 2013). Thus, we focused on these cognitive domains in this cross-sectional, community-based study of non-demented/non-depressed older adults. We specifically examined whether CVD-RFs are associated with structural connectivity in key brain regions associated with cardiovascular health and AD (Beauchet et al., 2013; Boots et al., 2015; Cardenas et al., 2012; Dickerson et al., 2009; Glodzik et al., 2012; Lamar et al., 2012; Moulton et al., 2015; Pini et al., 2016) and if this connectivity mediates the well-established link between CVD-RFs and cognition. We hypothesized that higher CVD-RFs will be associated with lower local efficiency, i.e., path length across nodes within a region, and lower nodal strength, i.e., the sum of the weights of the paths connected to a node. We further hypothesized that efficiency and nodal strength metrics will mediate the relationship between cumulative CVD-RF burden and a priori chosen cognitive domains of executive function, attention and information processing, and memory.

2. Material and methods

2.1. Participants

Participant data for this study came from a larger study of healthy aging and CVD-RFs at the University of Illinois at Chicago (UIC) Department of Psychiatry. The study was approved by the UIC Institutional Review Board (IRB) and conducted in accordance with the Declaration of Helsinki with written informed consent obtained from all participants. This study has also been approved by the Rush University Medical Center IRB with all requisite data use agreements in place prior to data analysis. Research data is confidential given that we do not have participant approval to share data with outside investigators; however, all code relevant to this study is available upon request.

Interested individuals underwent a brief telephone screening to determine initial study eligibility. At this screen, exclusion criteria consisted of self-reported current or past history of neurological conditions including AD or any other form of dementia or mild cognitive impairment, Parkinson's disease or any other movement disorder, stroke, or seizure disorder, current or past history of Axis I or II disorders (e.g., depression or bipolar disorder), a history of head injury or loss of consciousness, a present or past history of substance abuse or dependence, psychotropic medication use, or contraindications for magnetic resonance imaging (MRI) including metallic implants. A self-reported history of stable (e.g., diabetes) or remitted medical illness (e.g., cancer) was not an exclusionary factor. Individuals were not eligible for this study if they had received cognitive testing within the past year, or if they reported current involvement in a study with cognitive testing.

Individuals who passed this initial screen were then scheduled for a more intensive evaluation of inclusion and exclusion criteria. This evaluation consisted of affective and cognitive screens including the Structured Clinical Interview for DSM-IV-TR (SCID; First et al., 2002) and the Mini Mental State Examination (MMSE; Folstein et al., 1975). These screening measures were administered by a trained research assistant, and were followed by a blinded evaluation by a psychiatrist, who completed the 17-item Hamilton Depression Rating Scale (HAM-D; Hamilton, 1960). Participants were also asked about subjective memory impairment (SMI) during this time.

Final inclusion criteria consisted of an absence of psychiatric symptoms based on the SCID, a score $\leq$8 on the HAM-D, an MMSE score $\geq$24, as well as an absence of SMI. All study participants completed the Beck Depression Inventory (BDI; Beck et al., 1996) as well as the Beck Anxiety Inventory (BAI; Beck and Steer, 1990) for a subjective measure of depressive and anxiety symptomatology, respectively. In total, 121 individuals met final inclusion criteria for the overall study. Ten participants received their evaluations in Spanish and were excluded given that not all aspects of the cognitive assessment outlined below were English/Spanish compatible. This left 111 potential participants for the current study.

2.2. Study protocol

2.2.1. Cardiovascular disease risk factor (CVD-RF) assessment

Participants underwent a CVD-RF assessment with a registered nurse in the Center for Clinical and Translational Science's Clinical Research Center (CRC) at UIC. This evaluation consisted of a medical history and physical examination, in addition to two seated blood pressure readings separated by 5 min and an electrocardiogram. A 12-h fasting blood draw for quantification of glucose, hemoglobin A1c, lipid profiles, and other blood-based biomarkers was also performed. Given our interest in the impact of CVD-RF burden on tract-based structural connectivity and cognition, we chose to use a comprehensive measure of risk, namely the Framingham Stroke Risk Profile (FSRP). The FSRP is a widely-used measure of cardiovascular risk that has recently been revised from its

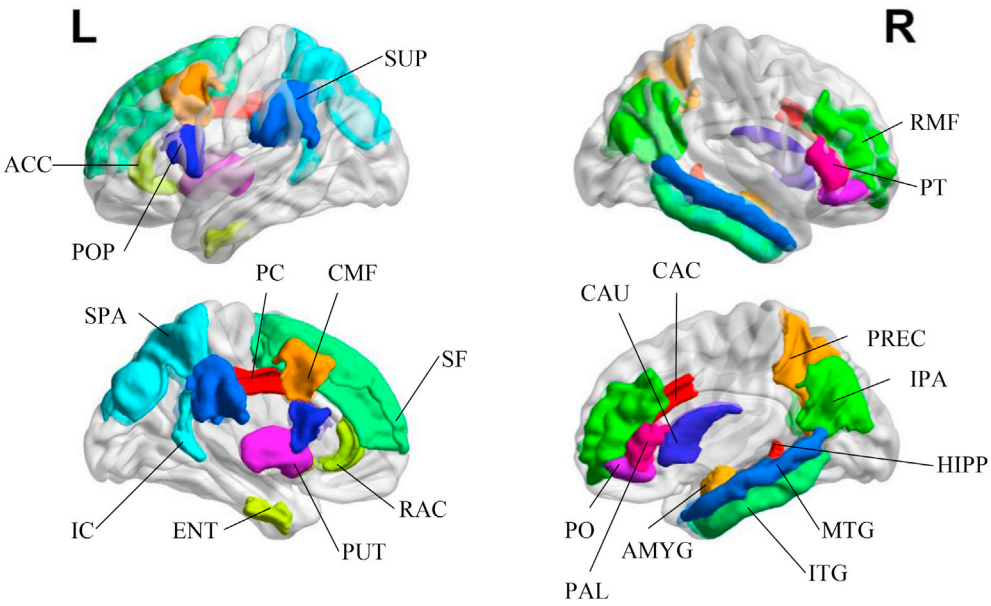

Fig. 1. Gray matter regions of interest associated with both cardiovascular risk factors and dementia. Colors do not necessarily delineate specific brain regions, as some colors were used more than once in identifying regions of interest. ACC = accumbens area; AMYG = amygdala; CAC = caudal anterior cingulate; CAU = caudate; CMF = caudal middle frontal gyrus; ENT = entorhinal cortex; HIPP = hippocampus; IC = isthmus cingulate; IPA = inferior parietal cortex; ITG = inferior temporal gyrus; MTG = middle temporal gyrus; PAL = pallidum; PC = posterior cingulate; PO = pars orbitalis; POP = pars opercularis; PREC = precuneus; PT = pars triangularis; PUT = putamen; RAC = rostral anterior cingulate; RMF = rostral middle frontal gyrus; SF = superior frontal gyrus; SPA = superior parietal cortex; SUP = supramarginal gyrus.

original version (Wolf et al., 1991) to more accurately predict stroke risk in diverse populations at time 't' (Dufouil et al., 2017). The revised metric incorporates age, sex, systolic blood pressure, anti-hypertensive therapy, diabetes, smoking, cardiovascular disease, and atrial fibrillation which we used to calculate 10-year risk of stroke, i.e., t = 10 (FSRP-10; see Dufouil et al., 2017, for calculation specifics). FSRP-10 was log-transformed to normalize the FSRP-10 distribution.

2.2.2. Neuroimaging acquisition and processing

Participants underwent neuroimaging at UIC's Center for Magnetic Resonance Research. Whole brain images were acquired on a GE MR 750 Discovery 3T scanner (General Electric Health Care, Waukesha, WI) using an 8-channel head coil. Participants were positioned supine on the scanner table, with earplugs to improve patient comfort and foam pads to minimize head movement. Participants were instructed to remain still throughout the scan. Sequences relevant for the current analyses included high resolution three-dimensional T1-and T2-weighted images and diffusion MRI. The T1-weighted images were acquired using a Brain Volume (BRAVO) imaging sequence (field of view: FOV = 22 mm; voxel size = $0.42\times0.42\times1.5\,mm^3$; 120 contiguous axial slices; TR/TE = 1200 ms/5.3 ms; flip angle = 13°) for quantification of gray matter volumes. A set of multi-slice T2-weighted fluid-attenuated inversion recovery (FLAIR) images was acquired using a two-dimensional PROPELLER sequence (FOV = 22 cm, voxel size = $0.35\times0.35\times3.0\,mm^3$, 40 contiguous axial slices, TR/TI/TE = 9500 ms/2500 ms/93.3 ms, flip angle = 142.35°) for collection of WMH. Diffusion MRI images were acquired using 2-D spin-echo EPI sequence (FOV = 20 mm; voxel size = $0.78\times0.78\times3.0\,mm^3$; TR/TE = 5525/93.5 ms; flip angle = 90°) for measures of white matter integrity. Forty contiguous axial slices aligned to the AC-PC line were collected in 32 gradient directions with b = 1400 s/mm^2 and 6 baseline (b_0) images.

Described in detail elsewhere (Boyle et al., 2016), quantification of WMH first involved registering the T1-weighted BRAVO data for each participant to the T2-weighted FLAIR data using affine registration (FLIRT, FMRIB, University of Oxford, UK; Smith et al., 2004). Brains were extracted from the co-registered BRAVO and FLAIR image volumes (BET, FMRIB, University of Oxford, UK; Smith, 2002). WMHs were then automatically segmented using a support vector machine classifier considering both BRAVO and FLAIR information for each participant (WMLS, SBIA, University of Pennsylvania; Zacharaki et al., 2008). WMH volume was log-transformed to normalize the WMH distribution.

Structural connectivity networks were created using a pipeline that integrates a series of image processing and analysis techniques. First, T1-weighted images were used to generate label maps for volumetric segmentation using FreeSurfer 6.0 software (https://surfer.nmr.mgh.harvard.edu/; Dale et al., 1999; Fischl et al., 1999). Each label map was composed of 82 different gray matter regions of interest (ROI) using the Destrieux atlas (Desikan et al., 2006; Destrieux et al., 2010; Fischl et al., 2004). Intracranial volume (ICV) was also derived from FreeSurfer. Next, for computation of probabilistic tractography (see Zhan et al., 2015 for a more comprehensive description), diffusion MRI images were corrected for eddy current distortions and head motion using the FSL (https://fsl.fmrib.ox.ac.uk/fsl/; Jenkinson et al., 2012; Smith et al., 2004; Woolrich et al., 2009) eddy-correct tool (Andersson and Sotiropoulos, 2016) and the non-brain tissue was removed using FSL Brain Extraction Tool (BET; Smith, 2002). The gradient table was also corrected accordingly. Diffusion tensors at each voxel were then estimated using the FSL dtifit tool for calculation of three principal eigenvectors, and three eigenvalues, as well as fractional anisotropy (FA). Then, images were elastically registered to T1-weighted scans using an inverse consistent registration algorithm with a mutual information cost function via Advanced Normalization Tools (ANTs; http://stnava.github.io/ANTs/; Avants et al., 2014), see Leow et al. (2007) and Zhan et al. (2015). In preparation for probabilistic tractography, we applied the FSL Bayesian Estimation of Diffusion Parameters Obtained using Sampling Techniques for modeling crossing fibers (Bedpostx; Behrens et al., 2007). This process uses Markov Chain Monte Carlo sampling to "build up distributions on diffusion parameters at each voxel" (https://fsl.fmrib.ox.ac.uk/fsl/); we modeled up to three fibers per voxel.

For construction of connectivity matrices, FSL Probtrackx (Behrens et al., 2003, 2007) was run on individual seed voxels with FA ≥ 0.2. Probtrackx repeatedly samples from the distributions of voxel-wise principal diffusion directions calculated from Bedpostx, each time computing probabilistic streamlines. Based on the provided data, this builds a distribution on the likely tract location and path in the matrix. One thousand iterations were run to ensure convergence of the Markov chains. Finally, the matrix was formed by detecting the number of fibers connecting ROI pairs determined from Probtrackx. The matrix is symmetric and has no self-connections (Zhan et al., 2013). Matrices were normalized by adjusting for the volume of individual ROIs. See Zhan and colleagues (Zhan et al., 2015) for additional information. Resulting weighted and undirected matrices were then analyzed in Brain Connectivity Toolbox (BCT; Rubinov and Sporns, 2010) as outlined below.

2.2.3. Neuroimaging analyses

In graph theory, a network is a set of 'nodes' or brain regions with 'edges' or connections between them, i.e., white matter tracts. For this study, we were interested in measures of local efficiency – a measure of the average inverse path length across nodes for a given region – and nodal strength – the sum of the weights of the paths connected to a node (Rubinov and Sporns, 2010). Each of these measures were extracted for analysis using BCT. Given that CVD-RFs as well as AD are known to negatively affect frontal, parietal, hippocampal, and other regions of the brain, we targeted specific ROIs (see Fig. 1) known to be affected by both CVD-RF burden as well as AD, including the superior frontal gyrus, inferior frontal gyrus (pars opercularis, pars triangularis, pars orbitalis), rostral and caudal middle frontal gyrus, caudal and rostral anterior, posterior, and isthmus cingulate cortex, entorhinal cortex, supramarginal gyrus, middle and inferior temporal gyrus, hippocampus, amygdala, superior and inferior parietal cortex, the basal ganglia (caudate, putamen, pallidum, and accumbens), and precuneus (Beauchet et al., 2013; Boots et al., 2015; Cardenas et al., 2012; Dickerson et al., 2009; Glodzik et al., 2012; Lamar et al., 2012; Moulton et al., 2015; Pini et al., 2016). Measures of the right and left hemisphere were analyzed separately.

2.2.4. Cognition

Participants underwent a comprehensive neuropsychological evaluation administered by trained research assistants supervised by a licensed clinical neuropsychologist. For this project, we focused on cognitive tests specifically associated with domains implicated in cardiovascular disease risk (DeRight et al., 2015). Principal Component Analysis (PCA) with Varimax Rotation was utilized to statistically group cognitive tests, with factor loadings >0.6 per rotated component included in resulting composite scores. In order to compute each composite score, relevant test scores were recoded such that "better" scores were higher (i.e., multiplied reversed variables by −1), and z-scores were computed for each cognitive variable. Finally, z-scores for the tests within each cognitive domain were averaged for all participants for a final composite measure of each cognitive domain of interest. The resultant cognitive domains, and their relevant tests, are as follows: *Executive Function* – Trail Making Test B minus A (Army Individual Test Battery, 1944), Letter Fluency (Benton and Hamsher, 1976), Letter Number Sequencing (Wechsler, 1997), and Matrix Reasoning (Wechsler, 1997); *Attention and Information Processing* – Trail Making Test A, Trail Making Test Motor (Army Individual Test Battery, 1944), and Digit Symbol Coding (Wechsler, 1997); *Memory* – California Verbal Learning Test —II (CVLT-II) Total Learning Trials 1–5, Delayed Free Recall, and Recognition Discriminability (Delis et al., 2000). Predicted verbal IQ (pVIQ) from the Wechsler Test of Adult Reading (Wechsler, 2001) was used as a measure of educational quality, as this is considered a more accurate means of assessing educational attainment rather than years of education in racially/ethnically diverse samples of older adults (Manly et al., 2002).

2.3. Statistical analyses

All analyses were conducted in SPSS Version 24, with $p \leq .05$ for significance. Multivariate linear regression was used to evaluate the associations between FSRP-10 and connectivity measures of local efficiency and nodal strength in key ROIs as listed in section 2.2.3. Covariates in this model included ICV, WMH (log-transformed), and educational quality as measured by pVIQ from the WTAR. Of note, age and sex were not included as covariates as they are adjusted for within the FSRP-10 calculation. Given we were testing pre-specified hypotheses, we did not correct for multiple comparisons as doing so may have decreased our power to detect true associations and increased the false negative rate (Rothman, 1990).

Mediation analysis examined whether brain connectivity in significant ROIs mediated the relationship between FSRP-10 and cognition using the PROCESS Macro for SPSS (Hayes, 2018). Specifically, simple mediation models (i.e., PROCESS Macro Model 4, seed = 100618) tested the direct effect of FSRP-10 on connectivity metrics (path a), the direct effect of connectivity metrics on cognition (path b), the direct effect of FSRP-10 on cognition (path c'), and the indirect effect of FSRP-10 on cognition via connectivity metrics (path ab), our effect of interest. The indirect effect was tested based on 5000 bootstrap iterations utilizing a 95% confidence interval (CI), with CI's not including zero indicating significance of the indirect effect. All models included ICV, WMH, and educational quality as covariates.

Table 1
Participant demographic information for full sample (n = 94).

Characteristic	Mean ± SD (Range)[a]
Age, years	68.16 ± 6.70 (60–89)
Female, %	52.1
Race/Ethnicity, %	
Non-Latinx White	45.7
Non-Latinx Black	46.8
Latinx	7.4
Right Handedness, %	90.4
Degree Years of Education	15.49 ± 2.67 (10–22)
HAM-D Total (n = 82)	1.13 ± 1.45 (0–7)
BDI Total	2.98 ± 3.17 (0–26)
BAI Total (n = 93)	2.49 ± 2.92 (0–11)
MMSE Total	28.72 ± 1.42 (25–30)

Latinx = Gender-neutral term for individuals with self-identified Hispanic/Latin ethnicity; HAM-D = Hamilton Depression Rating Scale; BDI = Beck Depression Inventory; BAI = Beck Anxiety Inventory; MMSE = Mini Mental State Examination.
[a] Values are Mean ± SD (Range) unless otherwise stated.

Table 2
Framingham Stroke Risk Profile component breakdown for full sample.

FSRP Discrete Variables	Present	Absent
Smoking	8.5%	91.5%
Cardiovascular disease	3.2%	96.8%
Atrial fibrillation	1.1%	98.9%
Age 65+	36.2%	63.8%
Diabetes mellitus, if age <65	0.0%	100.0%
Diabetes mellitus, if age 65+	10.6%	89.4%
Hypertension medication	42.6%	57.4%
FSRP Continuous Variables	**Men**	**Women**
Age, years	66.62 (6.29)	69.57 (6.82)
Systolic blood pressure, mmHg	136.78 (17.51)	136.89 (15.88)

FSRP = Framingham Stroke Risk Profile, mmHg = millimeter of mercury.

3. Results

3.1. Participant characteristics

Of the 111 potential participants for this study, 2 did not complete the entire behavioral protocol, 9 did not complete neuroimaging, 3 did not pass our MRI quality assurance procedures pertaining to the sequences needed for this study, and 3 had incidental findings; this brought our final analytic sample to 94. These 94 participants were, on average, 68 years of age, with approximately 15 years of education. Women comprised just over half of the sample, and nearly half of participants self-identified as Black. MMSE, HAM-D, and other screening measures of cognition and affect were all in the normal range, demonstrating the non-demented, non-depressed nature of this sample (see Table 1).

The majority of participants were not deemed to have most CVD-RFs included in the FSRP (i.e., smoking, cardiovascular disease, atrial fibrillation; see Table 2). They were, however, taking medication for hypertension (43%), and averaged 137 mmHg systolic blood pressure, meeting current criteria for hypertension (Whelton et al., 2018). Overall, the probability of stroke in the next 10 years for both women and men in this sample was 6%; this is consistent with average 10-year stroke risk probability found by Dufouil et al. (2017).

Table 3
The relationship between stroke risk and local nodal strength or efficiency while adjusting for educational quality and intracranial volume in a cross-sectional sample of older adults.

Region of Interest	Mean (SD)	β (SE)	t-value	p-value	partial η^2
Efficiency[a]					
Hippocampus (LH)	1.690 (.489)	-.329 (.164)	−2.009	.048	.043
Pars Opercularis (RH)	1.757 (.812)	-.538 (.264)	−2.042	.044	.045
Supramarginal Gyrus (RH)	1.235 (.400)	.366 (.129)	2.840	.006	.083
Nodal Strength					
Amygdala (LH)	.069 (.020)	-.014 (.007)	−2.007	.048	.043
Hippocampus (LH)	.172 (.053)	-.056 (.016)	−3.517	.001	.122
Hippocampus (RH)	.249 (.093)	-.085 (.029)	−2.873	.005	.085
Pars Triangularis (RH)	.058 (.018)	-.013 (.006)	−2.137	.035	.049
Rostral Middle Frontal Gyrus (LH)	.198 (.055)	-.046 (.018)	−2.475	.015	.064
Rostral Middle Frontal Gyrus (RH)	.197 (.051)	-.050 (.017)	−2.991	.004	.091
Thalamus (LH)	.161 (.042)	-.031 (.014)	−2.199	.030	.052
Thalamus (RH)	.191 (.051)	-.037 (.017)	−2.133	.036	.049

LH = left hemisphere; RH = right hemisphere.
[a] Efficiency variables were multiplied by a factor of 1000 for ease of interpretation of beta values.

3.2. Association between cardiovascular risk and structural connectivity

Linear regressions adjusted for ICV, WMH, and educational quality revealed significant associations between FSRP-10 and local efficiency within 3 of the 23 a priori ROIs, i.e., the left hippocampus, right pars opercularis, and right supramarginal gyrus (all p-values $\leq .05$). Higher 10-year stroke risk was associated with lower local efficiency with the exception of the right supramarginal gyrus, where higher 10-year stroke risk was associated with higher local efficiency (see Table 3 *and* Fig. 2).

Additionally, linear regressions adjusted for ICV, WMH, and educational quality indicated associations between FSRP-10 and local nodal strength in 8 of the 23 a priori ROIs, i.e., the left and right rostral middle frontal gyrus, left and right hippocampus, left and right thalamus, right pars triangularis, and left amygdala (all p-values $\leq .05$). In all associations, higher 10-year stroke risk was associated with lower nodal strength (see Table 3 *and* Fig. 2).

Due to the hypertensive nature of the sample, we were interested to see whether hypertension variables within the FSRP-10 were driving the aforementioned results. Thus, we re-ran the above analyses while only including the demographic and hypertension portions of the equation, i.e., age, sex, hypertension medication, and systolic blood pressure related variables. For local efficiency, results indicated that the right supramarginal gyrus retained significance ($p = .012$) while the right pars opercularis and left hippocampus did not (p's ≥ 0.054). For nodal strength, all results remained significant (p's < 0.050) with the exception of the right pars triangularis, right thalamus, and left amygdala (p's ≥ 0.082).

3.3. Mediation of structural connectivity on cardiovascular risk and cognition

Mediation analyses adjusting for ICV, WMH, and educational quality tested the indirect effect (i.e., path ab) of significant structural connectivity ROIs on the relationship between FSRP-10 and cognitive domains of memory, executive function, and attention/information processing. While mediation analyses of local efficiency yielded no significant findings, mediation of nodal strength on the FSRP-10 and cognition relationship was observed. Specifically, results revealed significant mediation of nodal strength in the left (indirect effect (ab): β (SE) = −.174 (0.108); 95% CI = [-0.423 to −0.001]) and right hippocampus (indirect effect (ab): β (SE) = −0.186 (0.105); 95% CI = [-0.423 to −0.020]) on the relationship between FSRP-10 and attention/information processing such that greater FSRP-10 was associated with lower strength in the hippocampus, which was in turn associated with poorer attention/information processing (see Fig. 3 and Supplementary Table S1). Results also revealed significant mediation of nodal strength in the left rostral middle frontal gyrus on the relationship between FSRP-10 and attention/information processing (indirect effect (ab): β

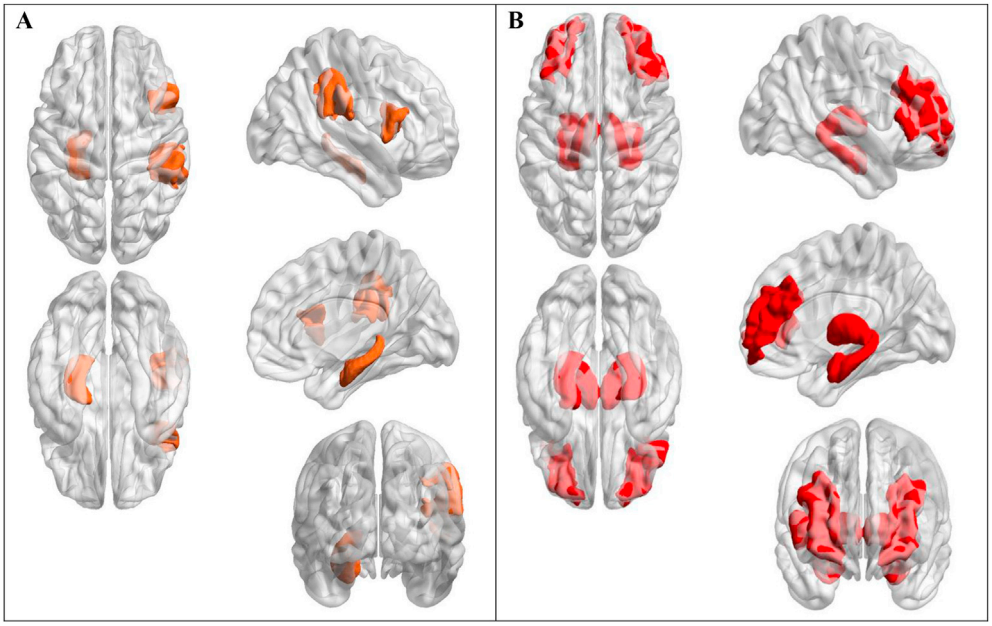

Fig. 2. Greater levels of CVD-RFS are associated with efficiency (orange) in the left hippocampus, right pars opercularis, right supramarginal gyrus, and nodal strength (red) in the left amygdala, bilateral hippocampus, right pars triangularis, bilateral rostral middle frontal gyrus, and bilateral thalamus.

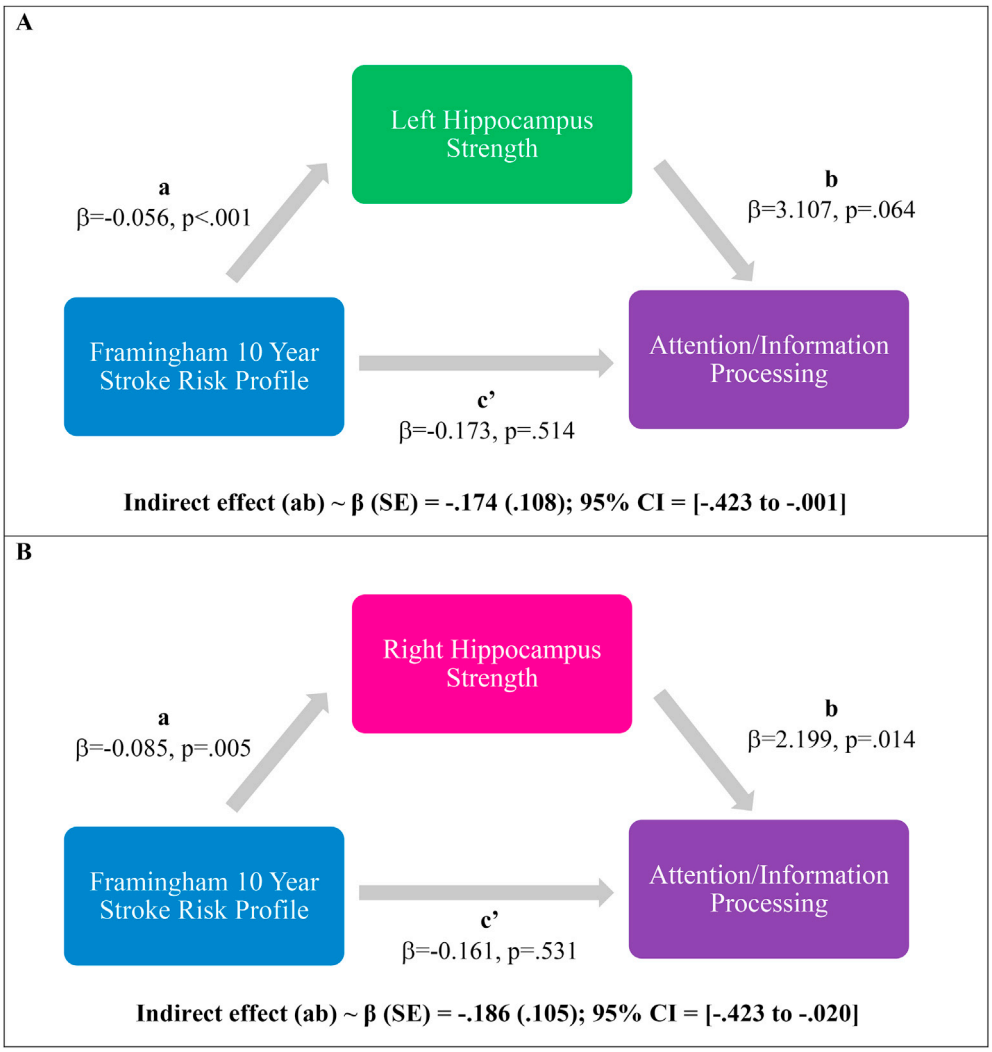

Fig. 3. Strength in the left (A) and right (B) hippocampus mediates the relationship between Framingham 10-year stroke risk and attention and information processing such that greater stroke risk associates with decreased strength, which in turn is associated with poorer performance on measures of attention and information processing.

(SE) = −0.146 (0.089); 95% CI = [-0.352 to −0.010]) and executive function (indirect effect (ab): β (SE) = −0.101 (0.062); 95% CI = [-0.241 to −0.001]). Again, results indicated that greater FSRP-10 was associated with lower strength in the left rostral middle frontal gyrus, which in turn was associated with poorer attention/information processing and executive function (see Fig. 4 and Supplementary Table S2). Given that these ROIs remained significant in the hypertension-only analyses above, we did not re-run these analyses with a reduced FSRP-10 equation.

4. Discussion

This study addresses the understudied relationship between CVD-RFs, cognition, and structural integrity of gray matter regions (cortical and subcortical) and their connecting white matter tracts. Our results indicate that CVD-RFs differentially impact the efficiency and nodal strength of the tract-based structural connectome within AD-associated regions. Specifically, higher 10-year stroke risk was associated with lower efficiency in the left hippocampus and right pars opercularis, and higher efficiency in the right supramarginal gyrus. Higher 10-year stroke risk was also associated with lower nodal strength in bilateral rostral middle frontal gyri, bilateral hippocampi, the thalamus bilaterally, right pars triangularis, and left amygdala. Additionally, nodal strength of both the left and right hippocampus mediated the association between FSRP-10 and attention and information processing, while nodal strength in the left rostral middle frontal gyrus mediated the association between FSRP-10 and attention and information processing, as well as executive function. Together, these findings suggest that CVD-RFs differentially impact efficiency and nodal strength of specific AD-related brain regions, which, in turn, are differentially related to specific cognitive domains in non-demented/non-depressed older adults.

While determining the underlying mechanisms for our differential results associating CVD-RFs and tract-based structural connectomics is beyond the scope of this cross-sectional study, existing literature points to several factors that may impact efficiency and nodal strength in affected regions. In addition to the role that CVD-RFs play in cortical gray matter thinning of our identified ROIs (Beauchet et al., 2013; Friedman et al., 2014; Leritz et al., 2011), associations between CVD-RF burden and nodal strength may also be due, in part, to the fact that white matter tracts permeating the identified regions are damaged, resulting in a breakdown in information transfer to associated gray matter regions. This damage may be caused by poor vasculature related to alterations in blood pressure (Leritz et al., 2011) and/or insulin receptor expression and inflammation related to diabetic symptomatology (Moulton et al., 2015). Of note and contrary to our hypothesis, the right supramarginal gyrus showed *greater* efficiency with higher CVD-RF burden; however, increases in local efficiency have been shown to occur in aging, likely due to compensation for

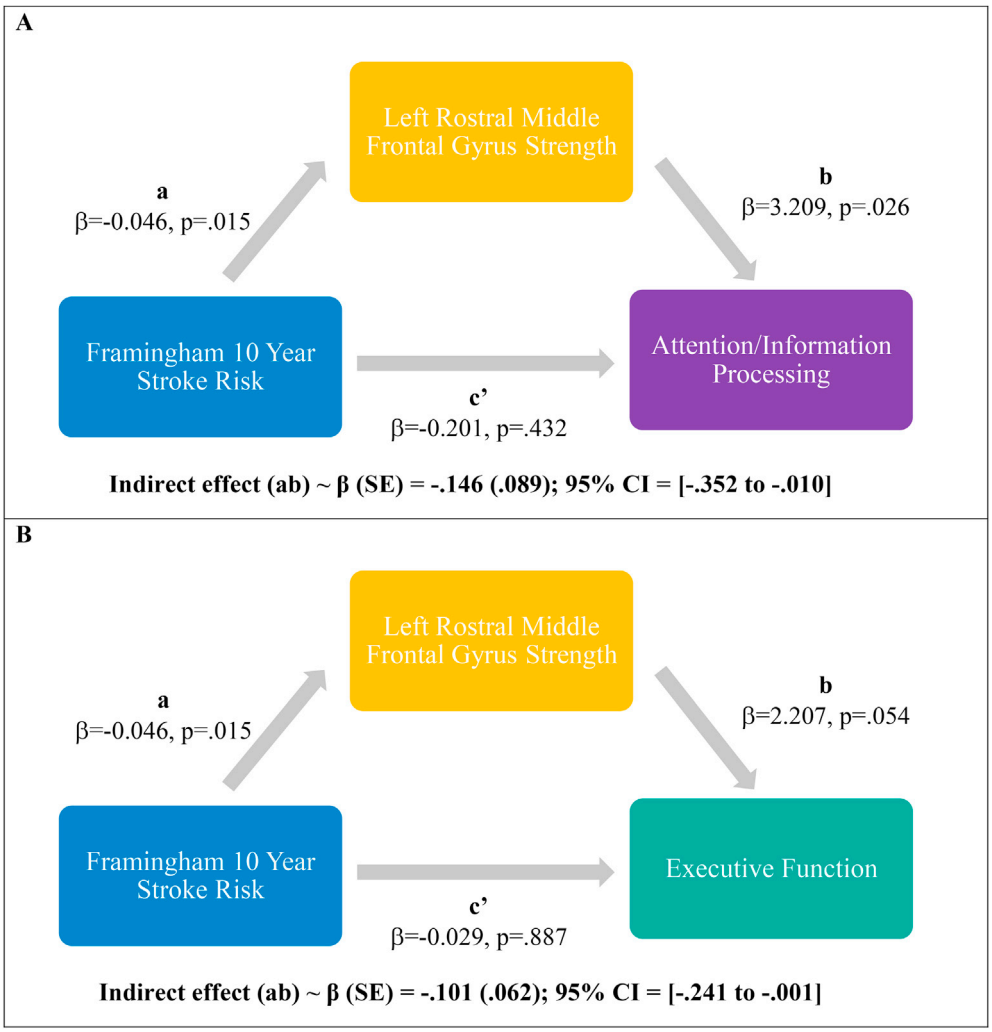

Fig. 4. Strength in the left rostral middle frontal gyrus mediates the relationship between Framingham 10-year stroke risk and attention and information processing (A) and executive function (B) such that greater stroke risk associates with decreased strength, which in turn is associated with poorer performance on measures of attention and information processing and executive function.

other altered brain regions (Barulli and Stern, 2013; Deslauriers et al., 2017). Ultimately, the underlying mechanisms for our results cannot be determined in this cross-sectional study, thus, longitudinal work is needed to more fully understand the interplay of efficiency and nodal strength as it relates to CVD-RF burden and cognition in aging.

Given the hypertensive nature of our sample, it was important to assess whether our results were driven by this particular CVD-RF. Indeed, results remained unchanged for several ROIs when utilizing a reduced, hypertension-specific equation that accounted for age and sex. These findings indicate that hypertension is a driving factor of nodal strength and efficiency connectivity patterns in several brain regions, consistent with literature investigating hypertension and individual gray and white matter regions (Beauchet et al., 2013; Kennedy and Raz, 2009). This is important to mention given the high prevalence of hypertension not only in our sample, but in the aging population more generally (Fryar et al., 2017). However, not all ROIs retained their significance when investigating hypertension specifically, implying that other CVD-RFs, such as diabetes and smoking, are likely contributing to the associations between CVD-RF burden and connectivity in other brain regions. Thus, a comprehensive evaluation of CVD-RF burden remains appropriate in relation to understanding cognition and brain aging.

Evidence for mediations of nodal strength, but not efficiency, on the relationship between CVD-RF burden and cognition suggest it is the path weights and not the path length that is associated with greater CVD-RF burden and subsequently alterations in cognition. Given our 23 ROIs, this appeared most relevant for bilateral hippocampi nodal strength and attention and information processing, as well as left rostral middle frontal gyrus nodal strength and attention and information processing and executive function. These findings integrate prior work in older adults reporting one-to-one relationships between hippocampal volume and CVD-RFs (Beauchet et al., 2013), nodal strength (Zhu et al., 2012), and attention (Aly and Turk-Browne, 2017) and information processing speed (O'Shea et al., 2016; Papp et al., 2014). They also extend previous findings showing relationships between greater CVD-RFs and less volume in the middle frontal gyrus (Leritz et al., 2011) and middle frontal gyrus neurodegeneration in aging (Samson and Barnes, 2013) that is associated with both attention (Japee et al., 2015) and executive dysfunction (Yuan and Raz, 2014). Taken together, disruption of the nodal strength of the hippocampus and rostral middle frontal gyrus may be caused by CVD-RFs' injurious effects on white matter near these regions, which slows communication throughout structural networks associated with attention and information processing and executive function (Aly and Turk-Browne, 2017; Samson and Barnes, 2013).

Strengths of this study include the use of tract-based structural connectomics to better understand the interplay between gray matter regions (cortical and subcortical) and their connecting white matter tracts

as it relates to CVD-RF and AD-related regions of interest. We utilized probabilistic tractography to allow for better delineation of crossing fibers in the brain, and ultimately a more accurate depiction of white matter tracts in regions with dense fiber connections (Zhan et al., 2015). Adjustment for WMH volumes in our analyses also strengthens our results, given the impact WMH can have on both structural connectivity and cognition (Langen et al., 2018). Additionally, this study utilized the most recent version of the FSRP (Dufouil et al., 2017), allowing for a more nuanced understanding of CVD-RFs and their combined influence on structural connectivity and cognition. Further, this work involved a racially and ethnically diverse cohort of non-demented/non-depressed older adults. Due to the cross-sectional nature of this study, however, we are unable to determine the direction of the relationships reported. Although we found associations with CVD-RFs and attention and information processing and executive function, we did not see similar relationships with memory as previously outlined in the literature using gray or white matter metrics. Nevertheless, our tract-based structural connectome findings provide not only better understanding of the interplay between gray matter regions (cortical and subcortical) and their connecting white matter as it relates to CVD-RF burden and brain aging, but also new insight into potential brain-mediated pathways by which CVD-RFs affect cognition.

5. Conclusions

Our work highlights the usefulness of tract-based structural connectomics to provide insight into the associations between CVD-RFs and brain-behavior relationships. Additionally, this work shows that there are detectable alterations in brain connectivity that associate with subtle alterations in cognitive function in the presence of CVD-RFs in non-demented/non-depressed older adults. If replicated and explored longitudinally, early detection of altered brain-behavior relationships in the context of CVD-RFs could point toward biomarkers that may be useful targets in prevention studies against cognitive decline and AD. At a minimum, our results provide support for the fact that CVD-RFs interact with brain and cognitive health in the absence of gross cognitive impairment or dementia at preclinical time points during which interventions may still be possible against pathological aging including AD.

Acknowledgements and funding sources

The authors would like to thank the participants of this study. The authors have no conflicts of interest to report. This research was supported by the National Institutes of Health, National Institute on Aging [K01 AG040192, R21 AG048176]. Additionally, aspects of this project were supported by the National Center for Advancing Translational Sciences and National Center for Research Resources, National Institutes of Health [UL1TR002003, 1S10RR028898].

Appendix A. Supplementary data

Supplementary data to this article can be found online at https://doi.org/10.1016/j.neuroimage.2019.04.024.

References

Aly, M., Turk-Browne, N.B., 2017. How hippocampal memory shapes, and is shaped by, attention. In: Hannula, D.E., Duff, M.C. (Eds.), The Hippocampus from Cells to Systems: Structure, Connectivity, and Functional Contributions to Memory and Flexible Cognition. Springer International Publishing, Cham, pp. 369–403.

Andersson, J.L.R., Sotiropoulos, S.N., 2016. An integrated approach to correction for off-resonance effects and subject movement in diffusion MR imaging. Neuroimage 125, 1063–1078. https://doi.org/10.1016/j.neuroimage.2015.10.019.

Army Individual Test Battery, 1944. Manual of Directions and Scoring. War Department, Adjutant General's Office, Washington, D.C.

Avants, B.B., Tustison, N.J., Stauffer, M., Song, G., Wu, B., Gee, J.C., 2014. The Insight ToolKit image registration framework. Front. Neuroinf. 8, 44. https://doi.org/10.3389/fninf.2014.00044.

Barulli, D., Stern, Y., 2013. Efficiency, capacity, compensation, maintenance, plasticity: emerging concepts in cognitive reserve. Trends Cognit. Sci. 17 (10), 502–509. https://doi.org/10.1016/j.tics.2013.08.012.

Beauchet, O., Celle, S., Roche, F., Bartha, R., Montero-Odasso, M., Allali, G., Annweiler, C., 2013. Blood pressure levels and brain volume reduction: a systematic review and meta-analysis. J. Hypertens. 31 (8), 1502–1516. https://doi.org/10.1097/HJH.0b013e32836184b5.

Beck, A.T., Steer, R.A., 1990. Beck Anxiety Inventory Manual. Psychological Corporation, San Antonio, TX.

Beck, A.T., Steer, R.A., Brown, G.K., 1996. Manual for the Beck Depression Inventory-II. Psychological Corporation, San Antonio, TX.

Behrens, T.E., Berg, H.J., Jbabdi, S., Rushworth, M.F., Woolrich, M.W., 2007. Probabilistic diffusion tractography with multiple fibre orientations: what can we gain? Neuroimage 34 (1), 144–155. https://doi.org/10.1016/j.neuroimage.2006.09.018.

Behrens, T.E., Woolrich, M.W., Jenkinson, M., Johansen-Berg, H., Nunes, R.G., Clare, S., et al., 2003. Characterization and propagation of uncertainty in diffusion-weighted MR imaging. Magn. Reson. Med. 50 (5), 1077–1088. https://doi.org/10.1002/mrm.10609.

Benton, A.L., Hamsher, K. d. S., 1976. Multilingual Aphasia Examination. University of Iowa, Iowa City.

Boots, E.A., Schultz, S.A., Oh, J.M., Larson, J., Edwards, D., Cook, D., et al., 2015. Cardiorespiratory fitness is associated with brain structure, cognition, and mood in a middle-aged cohort at risk for Alzheimer's disease. Brain Imaging Behav 9 (3), 639–649. https://doi.org/10.1007/s11682-014-9325-9.

Boyle, P.A., Yu, L., Fleischman, D.A., Leurgans, S., Yang, J., Wilson, R.S., et al., 2016. White matter hyperintensities, incident mild cognitive impairment, and cognitive decline in old age. Ann Clin Transl Neurol 3 (10), 791–800. https://doi.org/10.1002/acn3.343.

Cardenas, V.A., Reed, B., Chao, L.L., Chui, H., Sanossian, N., DeCarli, C.C., et al., 2012. Associations among vascular risk factors, carotid atherosclerosis, and cortical volume and thickness in older adults. Stroke 43 (11), 2865–2870. https://doi.org/10.1161/STROKEAHA.112.659722.

Dale, A.M., Fischl, B., Sereno, M.I., 1999. Cortical surface-based analysis. I. Segmentation and surface reconstruction. Neuroimage 9 (2), 179–194. https://doi.org/10.1006/nimg.1998.0395.

de Groot, M., Ikram, M.A., Akoudad, S., Krestin, G.P., Hofman, A., van der Lugt, A., et al., 2015. Tract-specific white matter degeneration in aging: the Rotterdam study. Alzheimers Dement 11 (3), 321–330. https://doi.org/10.1016/j.jalz.2014.06.011.

Debette, S., Seshadri, S., Beiser, A., Au, R., Himali, J.J., Palumbo, C., et al., 2011. Midlife vascular risk factor exposure accelerates structural brain aging and cognitive decline. Neurology 77 (5), 461–468. https://doi.org/10.1212/WNL.0b013e318227b227.

Delis, D.C., Kramer, J.H., Kaplan, E., Ober, B.A., 2000. California verbal learning test. In: Adult Version. Manual, second ed. Psychological Corporation, San Antonio, TX.

DeRight, J., Jorgensen, R.S., Cabral, M.J., 2015. Composite cardiovascular risk scores and neuropsychological functioning: a meta-analytic review. Ann. Behav. Med. 49 (3), 344–357. https://doi.org/10.1007/s12160-014-9681-0.

Desikan, R.S., Segonne, F., Fischl, B., Quinn, B.T., Dickerson, B.C., Blacker, D., et al., 2006. An automated labeling system for subdividing the human cerebral cortex on MRI scans into gyral based regions of interest. Neuroimage 31 (3), 968–980. https://doi.org/10.1016/j.neuroimage.2006.01.021.

Deslauriers, J., Ansado, J., Marrelec, G., Provost, J.S., Joanette, Y., 2017. Increase of posterior connectivity in aging within the Ventral Attention Network: a functional connectivity analysis using independent component analysis. Brain Res. 1657, 288–296. https://doi.org/10.1016/j.brainres.2016.12.017.

Destrieux, C., Fischl, B., Dale, A., Halgren, E., 2010. Automatic parcellation of human cortical gyri and sulci using standard anatomical nomenclature. Neuroimage 53 (1), 1–15. https://doi.org/10.1016/j.neuroimage.2010.06.010.

Dickerson, B.C., Bakkour, A., Salat, D.H., Feczko, E., Pacheco, J., Greve, D.N., et al., 2009. The cortical signature of Alzheimer's disease: regionally specific cortical thinning relates to symptom severity in very mild to mild AD dementia and is detectable in asymptomatic amyloid-positive individuals. Cerebr. Cortex 19 (3), 497–510. https://doi.org/10.1093/cercor/bhn113.

Dufouil, C., Beiser, A., McLure, L.A., Wolf, P.A., Tzourio, C., Howard, V.J., et al., 2017. Revised Framingham stroke risk profile to reflect temporal trends. Circulation 135 (12), 1145–1159. https://doi.org/10.1161/CIRCULATIONAHA.115.021275.

Elias, M.F., Sullivan, L.M., D'Agostino, R.B., Elias, P.K., Beiser, A., Au, R., et al., 2004. Framingham stroke risk profile and lowered cognitive performance. Stroke 35 (2), 404–409. https://doi.org/10.1161/01.STR.0000103141.82869.77.

Firbank, M.J., Wiseman, R.M., Burton, E.J., Saxby, B.K., O'Brien, J.T., Ford, G.A., 2007. Brain atrophy and white matter hyperintensity change in older adults and relationship to blood pressure. Brain atrophy, WMH change and blood pressure. J. Neurol. 254 (6), 713–721. https://doi.org/10.1007/s00415-006-0238-4.

First, M.B., Spitzer, R.L., Gibbon, M., Williams, J.B.W., 2002. Structured Clinical Interview for DSM-IV-TR Axis I Disorders, Research Version, Patient Edition with Psychotic Screen (SCID-I/P W/PSY SCREEN). Biometrics Research, New York State Psychiatric Institute, New York.

Fischl, B., Sereno, M.I., Dale, A.M., 1999. Cortical surface-based analysis. II: inflation, flattening, and a surface-based coordinate system. Neuroimage 9 (2), 195–207. https://doi.org/10.1006/nimg.1998.0396.

Fischl, B., van der Kouwe, A., Destrieux, C., Halgren, E., Segonne, F., Salat, D.H., et al., 2004. Automatically parcellating the human cerebral cortex. Cerebr. Cortex 14 (1), 11–22.

Folstein, M.F., Folstein, S.E., McHugh, P.R., 1975. "Mini-mental state". A practical method for grading the cognitive state of patients for the clinician. J. Psychiatr. Res. 12 (3), 189–198.

Friedman, J.I., Tang, C.Y., de Haas, H.J., Changchien, L., Goliasch, G., Dabas, P., et al., 2014. Brain imaging changes associated with risk factors for cardiovascular and cerebrovascular disease in asymptomatic patients. JACC Cardiovasc Imaging 7 (10), 1039–1053. https://doi.org/10.1016/j.jcmg.2014.06.014.

Fryar, C.D., Ostchega, Y., Hales, C.M., Zhang, G., Kruszon-Moran, D., 2017. Hypertension prevalence and control among adults: United States, 2015-2016. NCHS Data Brief (289), 1–8.

Gifford, K.A., Badaracco, M., Liu, D., Tripodis, Y., Gentile, A., Lu, Z., et al., 2013. Blood pressure and cognition among older adults: a meta-analysis. Arch. Clin. Neuropsychol. 28 (7), 649–664. https://doi.org/10.1093/arclin/act046.

Glodzik, L., Mosconi, L., Tsui, W., de Santi, S., Zinkowski, R., Pirraglia, E., et al., 2012. Alzheimer's disease markers, hypertension, and gray matter damage in normal elderly. Neurobiol. Aging 33 (7), 1215–1227. https://doi.org/10.1016/j.neurobiolaging.2011.02.012.

Gonzales, M.M., Ajilore, O., Charlton, R.C., Cohen, J., Yang, S., Sieg, E., et al., 2017. Divergent influences of cardiovascular disease risk factor domains on cognition and gray and white matter morphology. Psychosom. Med. 79 (5), 541–548. https://doi.org/10.1097/PSY.0000000000000448.

Hamilton, M., 1960. A rating scale for depression. J. Neurol. Neurosurg. Psychiatry 23, 56–62.

Hayes, A.F., 2018. Introduction to Mediation, Moderation, and Conditional Process Analysis : a Regression-Based Approach, second ed. Guilford Press, New York.

Hoogenboom, W.S., Marder, T.J., Flores, V.L., Huisman, S., Eaton, H.P., Schneiderman, J.S., et al., 2014. Cerebral white matter integrity and resting-state functional connectivity in middle-aged patients with type 2 diabetes. Diabetes 63 (2), 728–738. https://doi.org/10.2337/db13-1219.

Iadecola, C., 2013. The pathobiology of vascular dementia. Neuron 80 (4), 844–866. https://doi.org/10.1016/j.neuron.2013.10.008.

Iadecola, C., Yaffe, K., Biller, J., Bratzke, L.C., Faraci, F.M., Gorelick, P.B., et al., 2016. Impact of hypertension on cognitive function: a scientific statement from the American heart association. Hypertension 68 (6), e67–e94. https://doi.org/10.1161/HYP.0000000000000053.

Jacobs, H.I., Leritz, E.C., Williams, V.J., Van Boxtel, M.P., van der Elst, W., Jolles, J., et al., 2013. Association between white matter microstructure, executive functions, and processing speed in older adults: the impact of vascular health. Hum. Brain Mapp. 34 (1), 77–95. https://doi.org/10.1002/hbm.21412.

Japee, S., Holiday, K., Satyshur, M.D., Mukai, I., Ungerleider, L.G., 2015. A role of right middle frontal gyrus in reorienting of attention: a case study. Front. Syst. Neurosci. 9, 23. https://doi.org/10.3389/fnsys.2015.00023.

Jenkinson, M., Beckmann, C.F., Behrens, T.E., Woolrich, M.W., Smith, S.M., 2012. Fsl. Neuroimage 62 (2), 782–790. https://doi.org/10.1016/j.neuroimage.2011.09.015.

Kennedy, K.M., Raz, N., 2009. Pattern of normal age-related regional differences in white matter microstructure is modified by vascular risk. Brain Res. 1297, 41–56. https://doi.org/10.1016/j.brainres.2009.08.058.

Lamar, M., Charlton, R., Zhang, A., Kumar, A., 2012. Differential associations between types of verbal memory and prefrontal brain structure in healthy aging and late life depression. Neuropsychologia 50 (8), 1823–1829. https://doi.org/10.1016/j.neuropsychologia.2012.04.007.

Lamar, M., Rubin, L.H., Ajilore, O., Charlton, R., Zhang, A., Yang, S., et al., 2015. What metabolic syndrome contributes to brain outcomes in African American & caucasian cohorts. Curr. Alzheimer Res. 12 (7), 640–647.

Langen, C.D., Cremers, L.G.M., de Groot, M., White, T., Ikram, M.A., Niessen, W.J., Vernooij, M.W., 2018. Disconnection due to white matter hyperintensities is associated with lower cognitive scores. Neuroimage 183, 745–756. https://doi.org/10.1016/j.neuroimage.2018.08.037.

Leow, A.D., Yanovsky, I., Chiang, M.C., Lee, A.D., Klunder, A.D., Lu, A., et al., 2007. Statistical properties of Jacobian maps and the realization of unbiased large-deformation nonlinear image registration. IEEE Trans. Med. Imaging 26 (6), 822–832. https://doi.org/10.1109/TMI.2007.892646.

Leritz, E.C., Salat, D.H., Williams, V.J., Schnyer, D.M., Rudolph, J.L., Lipsitz, L., et al., 2011. Thickness of the human cerebral cortex is associated with metrics of cerebrovascular health in a normative sample of community dwelling older adults. Neuroimage 54 (4), 2659–2671. https://doi.org/10.1016/j.neuroimage.2010.10.050.

Li, X., Liang, Y., Chen, Y., Zhang, J., Wei, D., Chen, K., et al., 2015. Disrupted frontoparietal network mediates white matter structure dysfunction associated with cognitive decline in hypertension patients. J. Neurosci. 35 (27), 10015–10024. https://doi.org/10.1523/JNEUROSCI.5113-14.2015.

Llewellyn, D.J., Lang, I.A., Xie, J., Huppert, F.A., Melzer, D., Langa, K.M., 2008. Framingham Stroke Risk Profile and poor cognitive function: a population-based study. BMC Neurol. 8, 12. https://doi.org/10.1186/1471-2377-8-12.

Manly, J.J., Jacobs, D.M., Touradji, P., Small, S.A., Stern, Y., 2002. Reading level attenuates differences in neuropsychological test performance between African American and White elders. J. Int. Neuropsychol. Soc. 8 (3), 341–348.

McEvoy, L.K., Fennema-Notestine, C., Eyler, L.T., Franz, C.E., Hagler Jr., D.J., Lyons, M.J., et al., 2015. Hypertension-related alterations in white matter microstructure detectable in middle age. Hypertension 66 (2), 317–323. https://doi.org/10.1161/HYPERTENSIONAHA.115.05336.

Meusel, L.A., Kansal, N., Tchistiakova, E., Yuen, W., MacIntosh, B.J., Greenwood, C.E., Anderson, N.D., 2014. A systematic review of type 2 diabetes mellitus and hypertension in imaging studies of cognitive aging: time to establish new norms. Front. Aging Neurosci. 6, 148. https://doi.org/10.3389/fnagi.2014.00148.

Moulton, C.D., Costafreda, S.G., Horton, P., Ismail, K., Fu, C.H., 2015. Meta-analyses of structural regional cerebral effects in type 1 and type 2 diabetes. Brain Imaging Behav 9 (4), 651–662. https://doi.org/10.1007/s11682-014-9348-2.

O'Shea, A., Cohen, R.A., Porges, E.C., Nissim, N.R., Woods, A.J., 2016. Cognitive aging and the Hippocampus in older adults. Front. Aging Neurosci. 8, 298. https://doi.org/10.3389/fnagi.2016.00298.

Papp, K.V., Kaplan, R.F., Springate, B., Moscufo, N., Wakefield, D.B., Guttmann, C.R., Wolfson, L., 2014. Processing speed in normal aging: effects of white matter hyperintensities and hippocampal volume loss. Neuropsychol Dev Cogn B Aging Neuropsychol Cogn 21 (2), 197–213. https://doi.org/10.1080/13825585.2013.795513.

Pini, L., Pievani, M., Bocchetta, M., Altomare, D., Bosco, P., Cavedo, E., et al., 2016. Brain atrophy in Alzheimer's Disease and aging. Ageing Res. Rev. 30, 25–48. https://doi.org/10.1016/j.arr.2016.01.002.

Roberts, R.O., Knopman, D.S., Przybelski, S.A., Mielke, M.M., Kantarci, K., Preboske, G.M., et al., 2014. Association of type 2 diabetes with brain atrophy and cognitive impairment. Neurology 82 (13), 1132–1141. https://doi.org/10.1212/WNL.0000000000000269.

Rothman, K.J., 1990. No adjustments are needed for multiple comparisons. Epidemiology 1 (1), 43–46.

Rubinov, M., Sporns, O., 2010. Complex network measures of brain connectivity: uses and interpretations. Neuroimage 52 (3), 1059–1069. https://doi.org/10.1016/j.neuroimage.2009.10.003.

Samson, R.D., Barnes, C.A., 2013. Impact of aging brain circuits on cognition. Eur. J. Neurosci. 37 (12), 1903–1915. https://doi.org/10.1111/ejn.12183.

Smith, S.M., 2002. Fast robust automated brain extraction. Hum. Brain Mapp. 17 (3), 143–155. https://doi.org/10.1002/hbm.10062.

Smith, S.M., Jenkinson, M., Woolrich, M.W., Beckmann, C.F., Behrens, T.E., Johansen-Berg, H., et al., 2004. Advances in functional and structural MR image analysis and implementation as FSL. Neuroimage 23 (Suppl. 1), S208–S219. https://doi.org/10.1016/j.neuroimage.2004.07.051.

Wang, R., Fratiglioni, L., Laukka, E.J., Lovden, M., Kalpouzos, G., Keller, L., et al., 2015. Effects of vascular risk factors and APOE epsilon4 on white matter integrity and cognitive decline. Neurology 84 (11), 1128–1135. https://doi.org/10.1212/WNL.0000000000001379.

Wechsler, D., 1997. WAIS-III: Wechsler Adult Intelligence Scale. Psychological Corporation, San Antonio, TX.

Wechsler, D., 2001. Wechsler Test of Adult Reading: WTAR. Psychological Corporation, San Antonio, TX.

Whelton, P.K., Carey, R.M., Aronow, W.S., Casey Jr., D.E., Collins, K.J., Dennison Himmelfarb, C., et al., 2018. ACC/aha/aapa/abc/acpm/ags/APhA/ash/aspc/nma/pcna guideline for the prevention, detection, evaluation, and management of high blood pressure in adults: executive summary: a report of the American college of cardiology/American heart association task force on clinical practice guidelines. Hypertension 71 (6), 1269–1324. https://doi.org/10.1161/HYP.0000000000000066, 2017.

Wiseman, R.M., Saxby, B.K., Burton, E.J., Barber, R., Ford, G.A., O'Brien, J.T., 2004. Hippocampal atrophy, whole brain volume, and white matter lesions in older hypertensive subjects. Neurology 63 (10), 1892–1897.

Wolf, P.A., D'Agostino, R.B., Belanger, A.J., Kannel, W.B., 1991. Probability of stroke: a risk profile from the Framingham study. Stroke 22 (3), 312–318.

Woolrich, M.W., Jbabdi, S., Patenaude, B., Chappell, M., Makni, S., Behrens, T., et al., 2009. Bayesian analysis of neuroimaging data in FSL. Neuroimage 45 (1 Suppl. l), S173–S186. https://doi.org/10.1016/j.neuroimage.2008.10.055.

Yuan, P., Raz, N., 2014. Prefrontal cortex and executive functions in healthy adults: a meta-analysis of structural neuroimaging studies. Neurosci. Biobehav. Rev. 42, 180–192. https://doi.org/10.1016/j.neubiorev.2014.02.005.

Zacharaki, E.I., Kanterakis, S., Bryan, R.N., Davatzikos, C., 2008. Measuring brain lesion progression with a supervised tissue classification system. Med Image Comput Comput Assist Interv 11 (Pt 1), 620–627.

Zhan, L., Jahanshad, N., Jin, Y., Toga, A.W., McMahon, K.L., Zubicaray, G. I. d., et al., 2013. Brain network efficiency and topology depend on the fiber tracking method: 11 tractography algorithms compared in 536 subjects. In: Paper Presented at the 2013 IEEE 10th International Symposium on Biomedical Imaging, 7-11 April 2013.

Zhan, L., Zhou, J., Wang, Y., Jin, Y., Jahanshad, N., Prasad, G., et al., 2015. Comparison of nine tractography algorithms for detecting abnormal structural brain networks in Alzheimer's disease. Front. Aging Neurosci. 7, 48. https://doi.org/10.3389/fnagi.2015.00048.

Zhu, W., Wen, W., He, Y., Xia, A., Anstey, K.J., Sachdev, P., 2012. Changing topological patterns in normal aging using large-scale structural networks. Neurobiol. Aging 33 (5), 899–913. https://doi.org/10.1016/j.neurobiolaging.2010.06.022.